



Pharmaceutical Nanotechnology

Gelatin-coated magnetic iron oxide nanoparticles as carrier system: Drug loading and *in vitro* drug release studyBabita Gaihre^a, Myung Seob Khil^{b,c}, Douk Rae Lee^c, Hak Yong Kim^{b,c,*}^a Department of Bionanosystem Engineering, Chonbuk National University, Chonju 561-756, Republic of Korea^b Center for Healthcare Technology Development, Chonbuk National University, Chonju 561-756, Republic of Korea^c Department of Textile Engineering, Chonbuk National University, Chonju 561-756, Republic of Korea

ARTICLE INFO

Article history:

Received 1 June 2008

Received in revised form 28 July 2008

Accepted 18 August 2008

Available online 23 August 2008

Keywords:

Gelatin

Magnetic iron oxide

Coating

Doxorubicin hydrochloride

Encapsulation efficiency

pH responsive drug release

ABSTRACT

Magnetic iron oxide nanoparticles (IOPs) were coated with gelatin A and B and drug-loading efficiency was investigated using doxorubicin (DXR) as a model drug to evaluate their potential as a carrier system for magnetic drug targeting. Drug loading to coated IOPs was done using adsorption as well as desolvation/cross-linking techniques to understand their role. Drug loading by adsorption technique was done by incubating mixture of coated IOPs and drug in various conditions of pH, DXR-to-coated IOPs ratio, gelatin types and IOPs amounts. Drug loading by desolvation/cross-linking technique was done by adding acetone and glutaraldehyde (GTA) to the mixture of coated IOPs and DXR. The results indicated involvement of electrostatic interaction during loading of DXR-to-coated IOPs. Compared to adsorption technique, desolvation/cross-linking technique improved the efficiency of drug loading regardless of type of gelatin used for the coating. The DXR-loaded particles showed pH responsive drug release leading to accelerate release of drug at pH 4 compared to pH 7.4.

Crown Copyright © 2008 Published by Elsevier B.V. All rights reserved.

1. Introduction

Magnetic drug targeting has been used to improve localized drug delivery to interstitial tumor targets. By the application of an external magnetic field, the magnetic drug carriers could be retained to achieve very high concentrations of the chemotherapeutic agent near the target site for a given period of time without any toxic effects to normal surrounding tissue or to the whole body (Roullin et al., 2002; Muniyandy et al., 2004). Furthermore, cytotoxic effects of a drug may be increased when hyperthermia is used in combination with several chemotherapeutic agents (Wiedemann et al., 1997; Herman, 1983). The combination of hyperthermia and chemotherapeutics to treat solid tumors has attracted much research activity.

Magnetic nanoparticles (IOPs) covered with a layer of biodegradable polymer shell or evenly distributed in the matrix of polymer nanoparticles have been reported to be effective magnetic drug carrier (Wilhelm et al., 2003; Gupta and Curtis, 2004; Petri et al., 2005; Shi and Chow, 2004). The polymer coatings have found to reduce aggregation problem of uncoated IOPs and lower toxicity. Such composites have been used to successfully deliver DNA, RNA, and other relatively small therapeutic molecules to tar-

get tissues by the use of external magnetic field (Gupta and Gupta, 2005).

Although many groups have investigated the use of various organic coatings as a means of optimizing the delivery of IOPs to or into cells but very few works have been done using gelatin as a coating material (Muniyandy et al., 2004). Gelatin is a protein derived from collagen and commonly used plasma expander. Some of the useful properties of gelatin include solubility, biodegradability, biocompatibility and pH-induced surface charge (Young et al., 2005). Presence of multifunctional groups, like $-NH_2$, $-COOH$, in the gelatin chain makes it a suitable candidate to bind with drug like doxorubicin (DXR) forming drug-polymer conjugate (Leo et al., 1997) or poly(ethylene glycol) to form reticulo-endothelial system (RES) evading conjugate (Kushibiki et al., 2004). Furthermore, cell surface and extracellular matrix contain fibronectin, which contain specific site for binding to cells and a range of macromolecules including collagen and gelatin (Engvall and Ruoslahti, 1977). Moreover, gelatin can be fabricated as microspheres, nanospheres depending on the technique used for the fabrication and found to enhance tumoral cell phagocytosis (Coester et al., 2006).

Furthermore, some recent experimental investigations of gelatin adsorption onto mica (Kamiyama and Israelachvili, 1992), phosphatidyl choline-coated silica (Kamyshny et al., 1999), fumed silicas (Mironyuk et al., 2001), carbon particles (Bele et al., 2002), and polystyrene latices (Hone et al., 2000) conclude that the irreversible adsorption of gelatin is possible in the liquid/solid

* Corresponding author. Tel.: +82 63 270 2351; fax: +82 63 270 2348.
E-mail address: khy@chonbuk.ac.kr (H.Y. Kim).

interface. Combination of complex interactions e.g., van der Waals interactions, hydrophobic interactions, and electrostatic interactions between oppositely charged surfaces and proteins as well as reduction of the amount of ordered structure (e.g., α -helix or β -sheet) due to adsorption-induced conformational changes (Malmsten, 1998) are considered to be the driving force for the protein adsorption to the solid surface.

All of the aforementioned properties make gelatin a useful candidate for the surface coating of IOPs. In the present paper, we report surface coating of IOPs with gelatin A and B and investigated the drug encapsulation efficiency of the coated IOPs under different experimental conditions. Mostly polymer–drug conjugates are prepared chemically by using desolvation/cross-linking technique (Weber et al., 2000; Maria et al., 2002; Muniyandy et al., 2004; Bajpai and Choubey, 2006) or physically by varying pH of the medium (Young et al., 2005; Tian et al., 2007). Both of the loading processes are investigated to see their effect on the loading efficiency. Furthermore, drug release profiles of the loaded particles are investigated in basic as well as acidic medium. The drug chosen for the study was doxorubicin (DXR) that is an anthracycline anti-neoplastic agent, commonly used in the treatment of neoplasms, including leukemias and lymphomas (Young et al., 1981).

2. Materials and methods

2.1. Materials

The starting materials were gelatin type A from porcine skin (~175 bloom, Sigma–Aldrich, USA), gelatin type B from bovine skin (~225 bloom, Sigma–Aldrich, USA), iron (III) chloride hexahydrate (Fisher Scientific, UK), iron (II) chloride tetrahydrate (Fisher Scientific, UK), sodium hydroxide (Fisher Scientific, UK), hydrochloric acid (Fluka, UK), acetone (Samchun Chemical, Korea), 25% glutaraldehyde (GTA) (Sigma–Aldrich, USA), doxorubicin (DXR) hydrochloride (Sigma–Aldrich, USA). Deionized water purged with nitrogen gas was used in all steps involved.

2.2. Surface coating of IOPs and characterization

The IOPs were synthesized by co-precipitation of the ferrous and ferric chloride solution in concentrated sodium hydroxide solution as reported earlier (Gaihre et al., 2008a,b). In this experiment, a stock solution of ferrous and ferric chloride solution having $\text{Fe}^{2+}/\text{Fe}^{3+}$ ion ratio equal to 0.5 (molar ratio) was prepared by dissolving required amount of the corresponding salts (Gaihre et al., 2008a,b) and same stock solution was used to precipitate IOPs. Briefly, 1 M NaOH and 12 ml gelatin solution (A or B, 5% (w/v), pH 5) were added to the ferrous and ferric chloride stock solution (0.5, 1 and 2 ml), simultaneously. The resulting black precipitates were stirred for further 30 min before magnetic collection. The precipitates were redispersed in 12 ml of deionized water with brief sonication and dialyzed against deionized water overnight. The homogenous dispersions of surface-coated IOPs were collected by removing the aggregates by centrifugation at 3000 rpm for 2 min. The product would be referred to as GIOIBPs-0.5, GIOIBPs-1, and GIOIBP-2 for gelatin B-coated IOPs and GIOIAPs-1, and GIOIAPs-2 for gelatin A-coated IOPs. The numbers in each of the name represent the corresponding volume of ferrous and ferric chloride solution used for the precipitation.

2.2.1. IOPs concentration

The IOPs concentration present on different samples of the surface-coated IOPs dispersion was estimated using inductively coupled plasma spectrometer (ICPS-7500, Shimadzu, Japan). Samples for ICPS analysis were prepared by treating 10 μl of the

dispersion with 20 μl of 35% HCl and diluting the resulting product to 10 ml by adding deionized water. The IOPs concentration (mg/ml) was calculated by using following relation (Gupta and Curtis, 2004).

1 particle of IOP = 62896 iron atoms

1 g of IOPs = 1.71×10^{17} particles

2.2.2. Gelatin concentration

The coated IOPs were collected from the ferrofluid using magnet and the thermogravimetric analysis was done to find percentage of gelatin adsorbed to the surface of the IOPs. Thermogravimetric analyzer (Pyris 1 TGA, PerkinElmer, USA), operating at a heating rate of $10^\circ\text{C min}^{-1}$, from room temperature to 700°C , under steady flow of nitrogen gas was used.

2.2.3. Particle size and surface charge

The hydrodynamic size and zeta potential of the samples were measured by using dynamic lights scattering technique (DLS, Malvern system 4700, Malvern, UK). Samples were prepared by diluting 20 μl of the dispersion to 1.5 ml with deionized water.

2.2.4. Morphology

The morphology of surface-coated IOPs was observed by transmission electron (BIO-TEM, H-7650, Hitachi, Japan) microscopy operating at 100 kV.

2.2.5. Surface functional group

The coated IOPs were collected from the ferrofluid using magnet and the surface modification was analyzed using fourier transform infrared (FT-IR, FTS 1000, Varian, USA) spectroscopy at 4 cm^{-1} resolution. The FTIR spectrum was measured in the $400\text{--}4000\text{ cm}^{-1}$ region for sample dispersed in KBr pellets.

2.2.6. Crystalline structure

The coated IOPs were collected from the ferrofluid using magnet and the crystalline structure was analyzed using X-ray diffraction techniques. X-ray diffractometer (XRD, Lad-X 600, Shimadzu, Japan) utilizing $\text{CuK}\alpha$ radiation ($\lambda = 1.54053\text{ \AA}$), operating at 30 mA and 40 kV, was used to investigate the crystalline phases. The scan rate and scan angle were fixed at 4° min^{-1} and $20\text{--}70\ 2\theta$ degree, respectively.

2.3. Drug loading into coated IOPs

Mostly polymer–drug conjugates are prepared either by adsorption by varying pH of the medium or chemically by using cross-linking agent. In present work both of the loading process were investigated to see their role on the loading.

2.3.1. Drug loading through adsorption

The drug loading through adsorption was done by incubating the doxorubicin (DXR) and the gelatin-coated IOPs in different experimental conditions. Briefly, both an aqueous dispersion of gelatin-coated IOPs and DXR was pre-warmed at 37°C , and mixed together with vortex mixing. After incubation for 1 h at 37°C in dark, the free drug was removed by dialysis against deionized water for 1 h. The drug-loaded nanoparticle dispersion was stored at 4°C for further analysis.

The adsorption process was done at various pH (4 and 7.2), DXR-to-coated IOPs ratios (0.01, 0.02, 0.03), IOPs concentrations, and gelatin types (A and B) to investigate their effect in loading efficiency.

To investigate the effect of pH, DXR-to-coated IOPs ratio and IOPs concentration was 0.02 and 8 mg ml⁻¹, respectively, and gelatin B-coated IOPs was used.

Similarly, to investigate the adsorption process at various DXR-to-coated IOPs ratios, the pH and IOPs concentration in the dispersion was 7.4 and 8 mg ml⁻¹ and gelatin B-coated IOPs was used.

To investigate the effect of IOPs concentration, the DXR-to-coated IOPs ratio and pH was 0.02 and 7.4, respectively, and both gelatin A- and B-coated IOPs were used.

2.3.2. Drug loading through desolvation/cross-linking

For drug loading through desolvation/cross-linking process, the mixture of coated IOPs and drug was incubated at 37 °C in dark as mentioned above. After incubation for 1 h as mentioned above, acetone was added to the dispersion (50 µl per ml) to induce the desolvation process followed by addition of glutaraldehyde (GTA) (4%, v/v, 10 µl per ml) for cross linking. The mixture was incubated for further 1 h at 37 °C in dark. Lastly acetone, unreacted GTA and unloaded drugs were removed by dialysis against deionized water for 1 h.

The drug-loading process was done at pH 7.4 and drug-to-coated IOPs ratio was adjusted to 0.02. The IOPs concentrations were 0.2 and 28 mg ml⁻¹ for gelatin B- and A-coated IOPs, respectively.

2.4. Encapsulation efficiency

The DXR content in the DXR-loaded nanoparticles was determined by using previously reported method (Leo et al., 1999). Briefly, DXR-loaded nanoparticles dispersion was mixed with enzyme to have DXR-loaded nanoparticles-to-enzyme ratio of 5:1 and the resulting dispersion was incubated for 5 h at 37 °C in dark. As DXR covalent coupling can be quantified as DXR equivalents using absorption at 480 nm, the DXR content after enzymatic degradation was determined spectrophotometrically at 480 nm. The solution obtained from the unloaded nanoparticles in the same experimental conditions was used as blank. DXR concentration in the nanoparticles was determined by measuring absorbance at 480 nm against a standard curve. The standard curve was constructed with different concentrations of DXR (0.01–8 µg ml⁻¹) dissolved in distilled water.

The encapsulation efficiency was calculated using flowing relation

$$E = \frac{Q_{\text{DXR}}}{Q_{\text{total}}} \times 100$$

where E is the percentage encapsulation of the coated IOPs, Q_{DXR} the quantity of drug encapsulated in coated IOPs (g) and Q_{total} is the quantity of drug added for encapsulation (g).

2.5. In vitro drug release

The *in vitro* release study of DXR-loaded nanoparticles was carried out at 37 °C under magnetic stirring in dark using dynamic dialysis technique. According to the technique, drug is firstly released from the coated IOPs into the donor solution contained in the dialysis bag. Subsequently, the drug can diffuse through the dialysis bag in the receiver solution, where the drug concentration is determined. The particles with encapsulation efficiency 39.4% were used for this analysis.

Briefly, the DXR-loaded nanoparticles dispersion (100 µl, donor solution) was kept in a dialysis membrane with a molecular weight cut-off of 12,000–14,000 Da and dialyzed against 20 ml buffer solution (pH 4 or 7.4, receiver solution). At a regular interval of time

1 ml of receiver solution was withdrawn and same volume of solution was replaced. Absorbance of the withdrawn receiver solution was measured at 480 nm using UV-visible spectrophotometer and concentration of DXR was calculated using the standard calibration curve. The solution obtained from a dialysis test carried out using unloaded nanoparticles was used as control. The cumulative fraction of release doxorubicin versus time was expressed by following equation

$$\text{Cumulative release DXR (\%)} = \frac{[\text{DXR}]_t}{[\text{DXR}]_{\text{total}}} \times 100$$

where $[\text{DXR}]_t$ is the amount of DXR released at time t , $[\text{DXR}]_{\text{total}}$ is the total DXR present in the DXR-loaded nanoparticles. To study the drug release in the presence of a proteolytic enzyme the dialysis test was performed for 30 h without enzyme as described above. After this time period, trypsin solution (DXR-loaded nanoparticles-to-enzyme ratio = 5:1) was added to the donor solution and analyzed as before.

3. Results and discussion

3.1. Characterization of surface modified IOPs

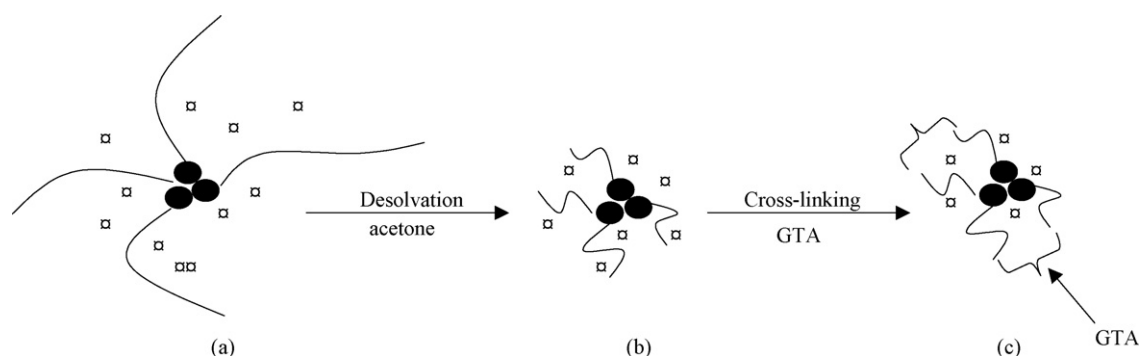
3.1.1. Physicochemical properties

Physicochemical properties of five different samples of stabilized ferrofluids were studied and the result is presented in Table 1. In this table first three samples (GIOIBPs-0.5, 1, and 2) represent gelatin B-stabilized ferrofluid and last two (GIOIBPs-1 and 2) represent gelatin A-stabilized ferrofluid. The table indicates that there was increase in IOPs concentration of the ferrofluid with increasing iron chloride stock solution for both types of gelatin coatings. Furthermore, with increasing IOPs amount, the amount of gelatin and hydrodynamic size of the ferrofluid decreased for both type of gelatin coatings. As in this experiment, gelatin amount was kept constant and with increasing IOPs amount in the ferrofluid we can expect increasing competition between each IOPs for fixed amount of gelatin resulting in decrease in gelatin layer adsorbed per IOPs as suggested by Table 1. Furthermore, in addition to imparting water solubility to the ferrofluid, gelatin has another important property i.e., gelatin solution converts to gel, which is marked by increasing viscosity. However, the time taken for a gelatin solution to convert to gel depends on the concentration of gelatin in the solution. The higher the concentration of gelatin, more viscous the solution would be and the faster it changes to gel. Particle size would be definitely larger in more viscous solution. Decreasing size of ferrofluid with decreasing gelatin, shown in Table 1, is as expected because it decreases the viscosity (Table 1) and gelling property of the ferrofluid.

Although, both types of ferrofluid i.e., gelatin A- as well as gelatin B-stabilized ferrofluid showed similar trend of decrease in hydrodynamic size of the ferrofluid with increasing IOPs amount, different trend of zeta-potential variation was observed for them. For example, gelatin B-stabilized ferrofluid showed increasing zeta potential (GIOIBPs-0.5 to GIOIBPs-2.0) but gelatin A-stabilized ferrofluid showed decreasing zeta potential with increasing IOPs amount of the ferrofluid (GIOIAPs-1.0 to GIOIAPs-2.0). Before zeta potential and size analysis, the pH of the dispersion was adjusted to 7.2. At this pH, since gelatin B and IOPs, both, would have negative charge, the more negative charge would be added to the ferrofluid when IOPs were coated with gelatin B. The decreasing gelatin layer in the IOPs surface (GIOIBPs-0.5 to GIOIBPs-2.0) would, ultimately, decrease the negative charge. On the other hand, gelatin A has neutral or slight positive charge at pH 7.2 (isoelectric point 7–9), it would neutralize the negative charge of IOPs leading to less negative zeta potential of gelatin A-coated IOPs. Increasing amount

Table 1
Physicochemical properties of gelatin coated IOPs

Samples	Liquid property	Viscosity (cP)	IOPs (mg/ml)	Gelatin (%)	Size (nm)	Zeta (mV)
GIOIBPs-0.5	Turns gel after 24 h	6	0.2	58	356.4	−185.1
GIOIBPs-1.0	Free-flowing liquid	4	8.0	57	288.0	−126.0
GIOIBPs-2.0	Free-flowing liquid	3	17.0	49	176.0	−46.6
GIOIAPs-1.0	Free-flowing liquid	4	9.0	59	301.2	−46.8
GIOIAPs-2.0	Free-flowing liquid	3	28.0	56	240.5	−126.3



Scheme 1. Absorption of gelatin layer to IOPs (●) surface (a), coiling of the gelatin chain due to addition of acetone (b), and cross-linking of gelatin chain with GTA, leading to encapsulation of drug (□) in gelatin-coated IOPs (c).

of IOPs in the dispersion (GIOIAPs-2.0 compared to GIOIAPs-1.0) decreased the amount of gelatin layer on the surface, as suggested by Table 1, which resulted in decrease in positive charge making the coated particle more negative. These changes in surface charge under different experimental condition confirmed that the IOPs-core was coated with gelatin layer forming core-shell structure as shown in Scheme 1a.

Furthermore, Table 1 indicates that gelatin A-stabilized ferrofluid had large amount of IOPs stabilized compared to gelatin B-stabilized ferrofluid, under similar condition. For colloidal stability, the repulsive forces between particles must be dominant and steric repulsion is one of the fundamental mechanisms that affect colloidal stability. The steric repulsion involves polymers added to the system adsorbing onto the particle surface forming a core-shell type structures and causing repulsion. As discussed in Section 1, gelatin is a natural polymer with carboxyl, amine, and amide functional groups present in the polymer chain. In addition, depending on the pH different charges could develop on these functional groups making gelatin negatively or positively charged (Young et

al., 2005). Before surface coating, the pH of the gelatin was adjusted to 5. As suggested by isoelectric point of B (isoelectric point 4.7–5.2) and gelatin A (isoelectric point 7–9), gelatin B would have neutral or slight positive charge and gelatin A would have comparatively large positive charge. Similarly, as IOPs were synthesized from the basic solution, it would have negative charge (Illes and Tombacz, 2006). So, adsorption of the gelatin to the IOPs in the dispersion could be visualized as shown in Scheme 1a, which was induced due to electrostatic interaction between the gelatin layer and IOPs surface. Since, gelatin A had more positive charge compared to gelatin B, the ferrofluid stabilized by gelatin A showed larger amount of stabilized IOPs (Table 1).

3.1.2. Morphology, functional group analysis and crystalline structure

The surface morphology, functional group and crystalline structure for gelatin B-coated IOPs were analyzed using BIO-TEM, FT-IR, and XRD and the results are presented as Figs. 1–3, respectively. The surface-coated IOPs were collected from the

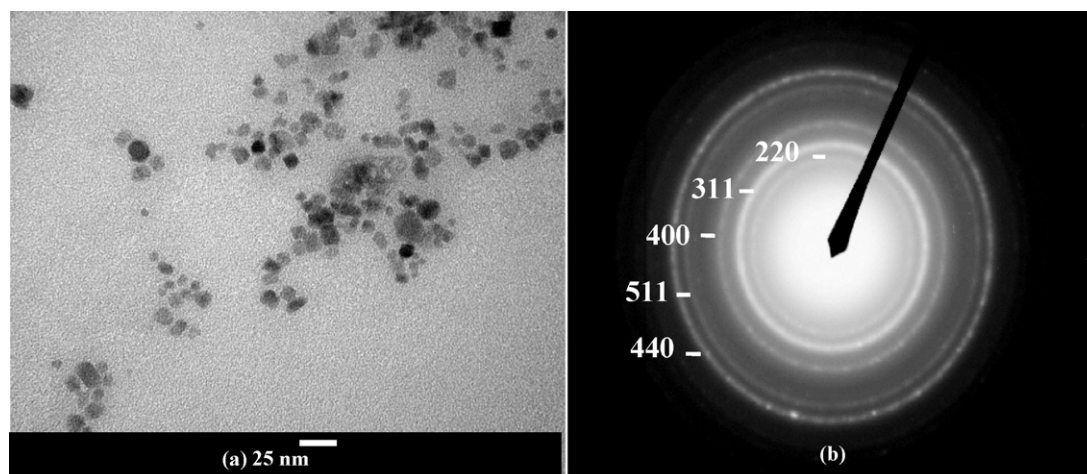


Fig. 1. BIO-TEM (a) and SADP (b) of coated IOPs.

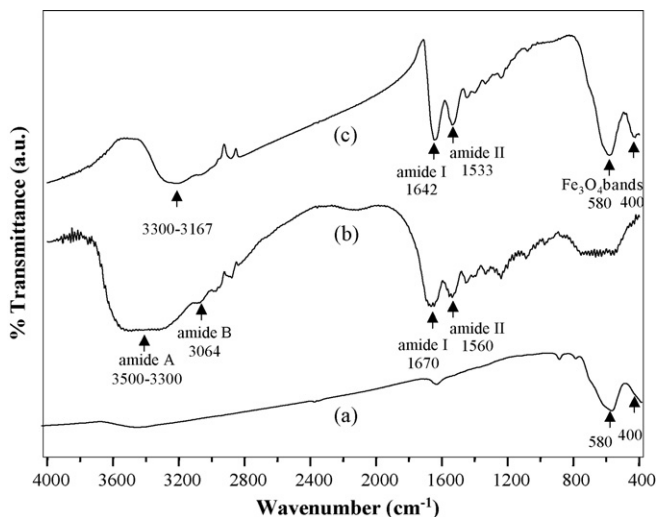


Fig. 2. FT-IR spectrum of uncoated IOPs (a), plain gelatin (b), and coated IOPs (c).

ferrofluid-using magnet and air-dried before analysis by FT-IR and XRD.

BIO-TEM (Fig. 1a) of gelatin B-coated IOPs indicated that the crystals were roughly spherical in shape with average crystal diameter in the narrow range of 5–13 nm. The narrow nanoparticle size range is an important requirement because uniform size particles provide an equal probability of magnetic capture and are characterized by similar drug content. The precipitation and simultaneous coating process of nanoparticles provided particles of narrow size range. The selected electron diffraction pattern (SADP) obtained from coated IOPs (Fig. 1b) consisted of five distinct concentric rings depicting the spinel crystal structure.

Fig. 2 represents the FT-IR spectrum of the coated IOPs along with plain gelatin and uncoated IOPs. The peaks at 580 and 400 cm^{-1} were the characteristic peaks for the IOPs (Gupta and Curtis, 2004). Similarly, the plain gelatin exhibited a number of characteristic spectral bands. The most characteristics of them were; N–H stretching at 3300–3500 cm^{-1} for amide A, C–H stretching at 3064 cm^{-1} for amide B, C=O stretching at 1670 cm^{-1} for amide I, N–H deformation at 1560 cm^{-1} for the amide II, and other bands associated with C–N stretching and N–H deformation for

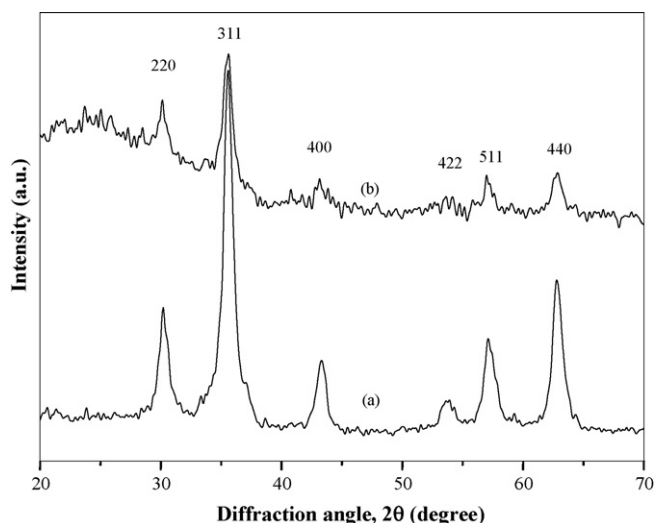


Fig. 3. XRD spectrum of uncoated IOPs (a) and coated IOPs (b).

amide III groups (Chang and Tanaka, 2002). All these characteristic bands were present in the spectrum for coated IOPs too. Moreover, the characteristic bands for IOPs were also seen in their usual positions at 580 and 400 cm^{-1} . The FT-IR indicated presence of polymer in IOPs surface.

The crystalline phases of the gelatin B-coated IOPs were characterized by observing XRD patterns of the sample (Fig. 3). The positions and relative intensities of the peaks at 2θ angles of 30.1, 35.5, 43.3, 53.4, 56.4, and 62.6 were quite similar to those of magnetite (Cornell and Schwertmann, 2000). Presence of oxygen could lead to oxidation of IOPs to haematite, ferric hydroxide and other phase of iron oxides. The XRD patterns ruled out presence of all these unwanted impurities.

3.2. Drug loading into coated IOPs

The drug loading to coated IOPs were done using adsorption and desolvation/cross-linking techniques.

3.2.1. Drug loading through adsorption

The pK_a of doxorubicin is 8.6, and protonated amino nitrogen provided the positive charge to the drug at pH 7.2 (Young et al., 1981). As suggested by Table 1, the surface charge of the coated IOPs would be negative at the given pH. So, the electrostatic interaction between coated IOPs and doxorubicin could be the basis for the drug binding.

Increasing zeta potential of surface coated IOPs after drug loading, as shown by Fig. 4a–c, indicated the interaction. After drug loading, as, the surface charge became more positive the surface layer would be pulled more strongly by negative core (IOPs, $\text{zeta} = -20$ mV) resulting in decreased size with increasing IOPs, as shown in Fig. 5b. Fig. 6 represents surface charge and size of the gelatin B-coated IOPs after drug loading with increasing drug-to-nanoparticle ratio. The increase in zeta potential and decrease in size with increasing drug-to-nanoparticle ratio after drug loading also indicate involvement of electrostatic interaction between drug and coated IOPs.

However, the gelatin B-coated IOPs in acidic medium (Fig. 5a) and gelatin A-coated IOPs in basic pH (Fig. 5c) showed unexpected increase in size after drug loading. In these two samples one thing was common i.e., both of the coated IOPs acquired positive zeta potential after drug loading (Fig. 4a and c). Tian et al. (2007) showed similar increase in size of the loaded particles in acidic pH due to aggregation, where both of the components acquired positive charge. We also strongly believe that with increasing positive charge aggregation of the coated IOPs might occurred resulting in increased hydrodynamic size.

3.2.1.1. Encapsulation efficiency. Figs. 7 and 8 represent the encapsulation efficiency of coated IOPs in different experimental conditions. Doxorubicin was added to the surface coated IOPs at different pH (4 and 7.2) and various drug-to-nanoparticle ratio (0.01, 0.02, and 0.03) and it was found that with increasing pH and drug-to-nanoparticle ratio the encapsulation efficiency also increased (Fig. 7a and b) as expected because increasing pH made the surface-coated IOPs more negative (Fig. 4a), thus, aiding the charge-induced adsorption of positive drug. However, since, increasing amount of IOPs in gelatin B-coated IOPs made them less negative (Table 1 and Fig. 4b), the encapsulation efficiency also decreased as shown in Fig. 8a. On the other hand, increasing encapsulation efficiency with increasing IOPs amount in gelatin A-coated IOPs as shown by Fig. 8b was as expected because increasing IOPs amount made gelatin A-coated IOPs more negative (Table 1 and Fig. 4c).

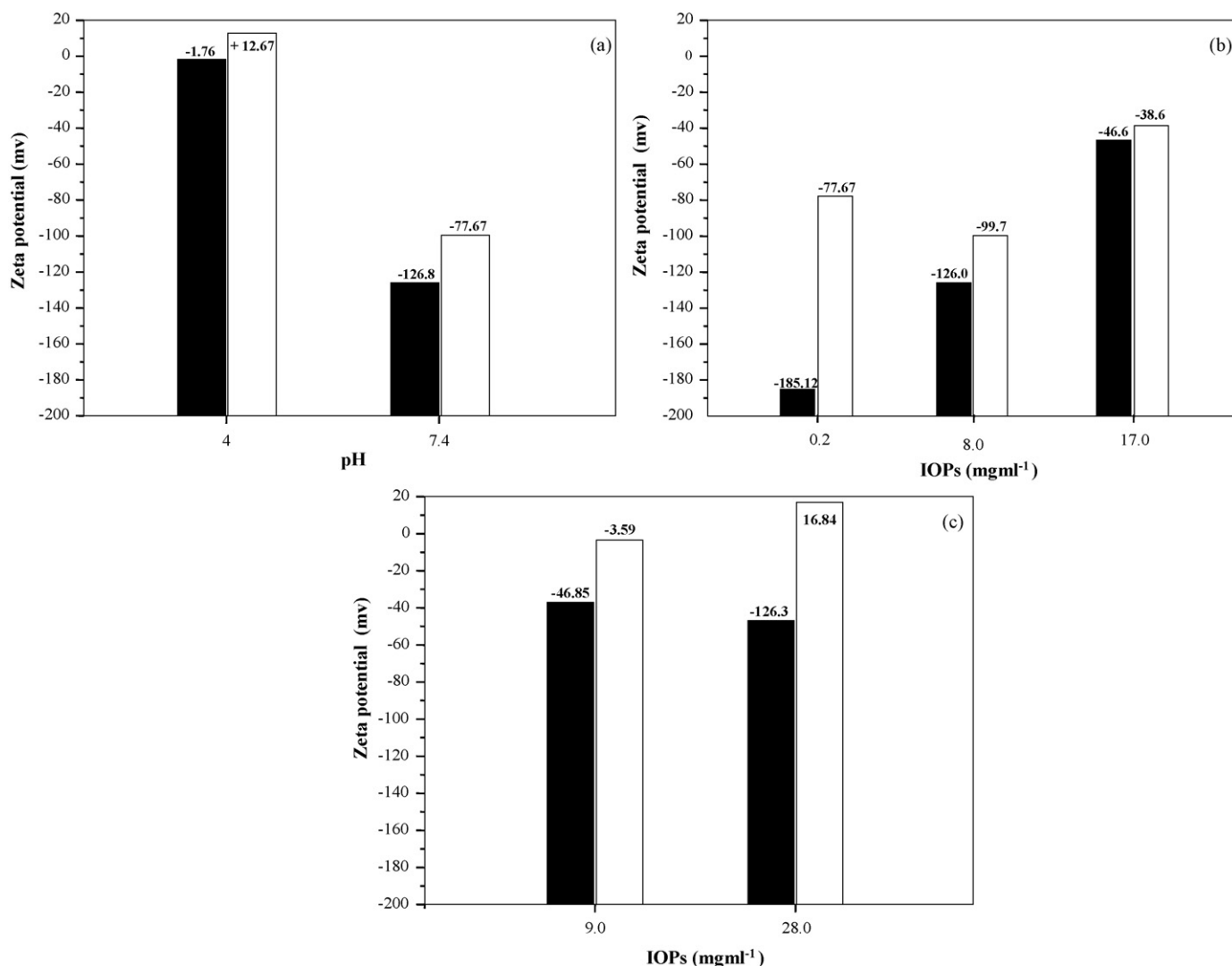


Fig. 4. Effects of pH (a) and IOPs concentration (b and c) on zeta potential of gelatin B (a and b) and A (c) coated IOPs before (■) and after (□) drug loading.

3.2.2. Drug loading through desolvation/cross-linking

Desolvation and cross-linking technique had been used to encapsulate drug. In this technique, the mixture of gelatin, IOPs and drug in aqueous solution was first treated with acetone followed by addition of glutaraldehyde (GTA) for desolvation and cross-linking purpose (Weber et al., 2000; Maria et al., 2002; Muniyandy et al., 2004; Bajpai and Choubey, 2006). Theoretically, when acetone is added to the surface-coated nanoparticle dispersion, coiling of the extended chain occurs because of insolubility of gelatin chain in acetone as shown in Scheme 1b. When GTA is added to the solution, it reacts with gelatin chain intermolecularly or intramolecularly leading to formation of gelatin-coated IOPs with different hydrodynamic size. If drug is present at this stage it is trapped in side the gelatin chain or conjugated intermolecularly to gelatin chain mediated with GTA as shown by Scheme 1.

Although the technique was conceptually simple, acetone and GTA amount was found to affect the size and stability of the coated IOPs (Gaihre et al., 2008a,b). So, exact amount of desolvating/cross-linking agent was optimized to get the coated IOPs of best size and stability before drug-loading experiment. From the optimization step we concluded that 50 μ l acetone and 10 μ l GTA per ml of coated IOPs dispersion and 1 h incubation time would be suitable parameters for the drug loading using desolvation and cross-linking

technique. Although both of gelatin A- and B-coated IOPs showed decrease in size after desolvation/cross-linking process as shown by Fig. 9a and b, there was no drastic change in size after drug loading.

3.2.2.1. Encapsulation efficiency. Fig. 10a and b make the comparison of encapsulation efficiency when drug loading was done by simple charge-induced adsorption and/or by desolvation/cross-linking technique and it was found that the later technique increased the loading efficiency (Fig. 10a and b) irrespective of type of gelatin used for coating.

3.3. In vitro drug release

3.3.1. In absence of enzyme

The drug release behavior of gelatin B-coated IOPs was investigated using a dialysis membrane in basic as well as acidic medium at 37 °C in dark. Fig. 11 shows the release profile of doxorubicin (DXR) in absence and presence of coated IOPs, which was used as a carrier system. The release profile of DXR from the coated IOPs was, further, compared using acidic (pH 4) and basic (pH 7.4) release medium.

It was apparent that almost 90% of the drug released within 4 h of dialysis, when pure DXR was dialyzed in basic medium (Fig. 11a).

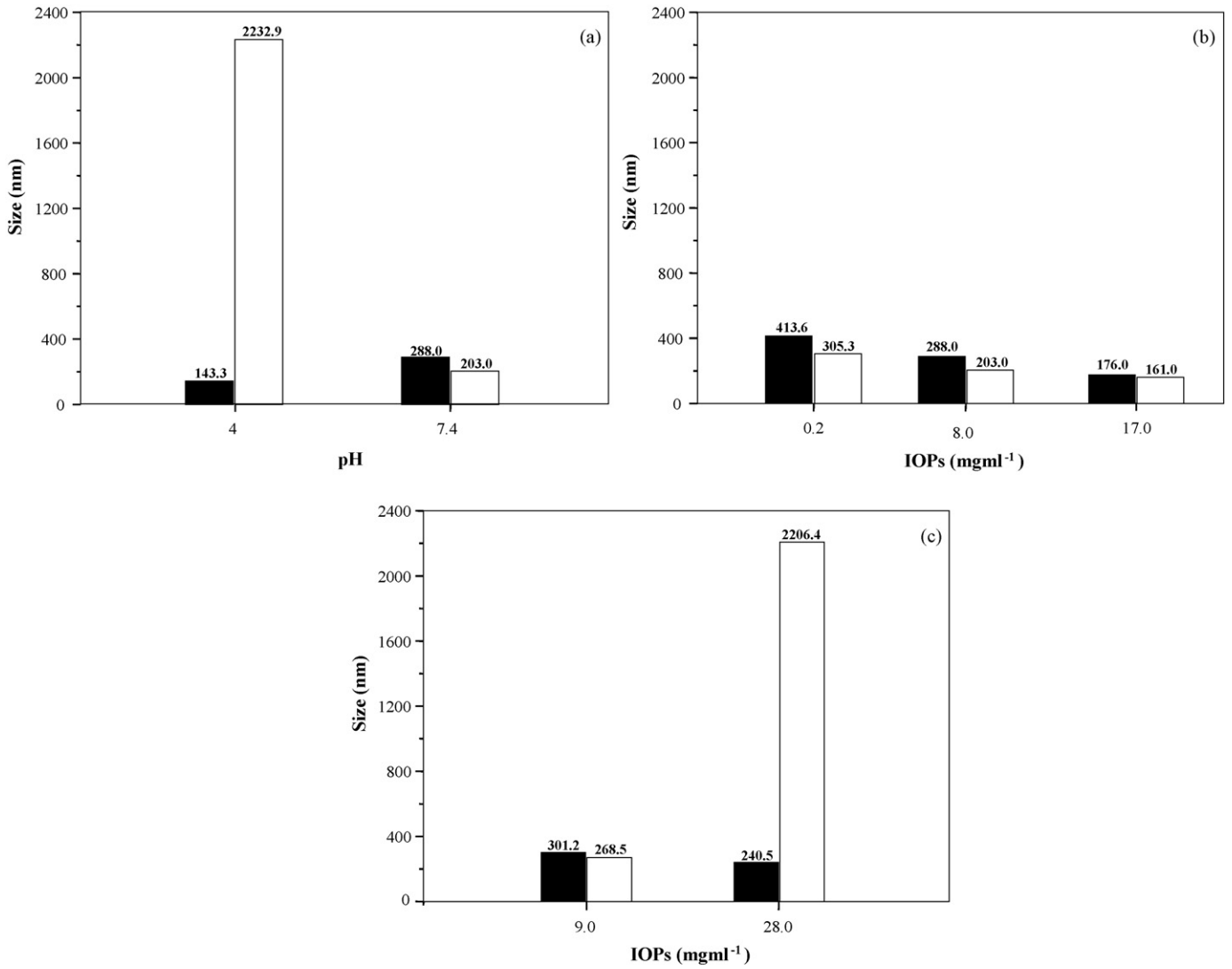


Fig. 5. Effects of pH (a) and IOPs concentration (b and c) on the size of gelatin B (a and b) and A (c) coated IOPs before (■) and after (□) drug loading.

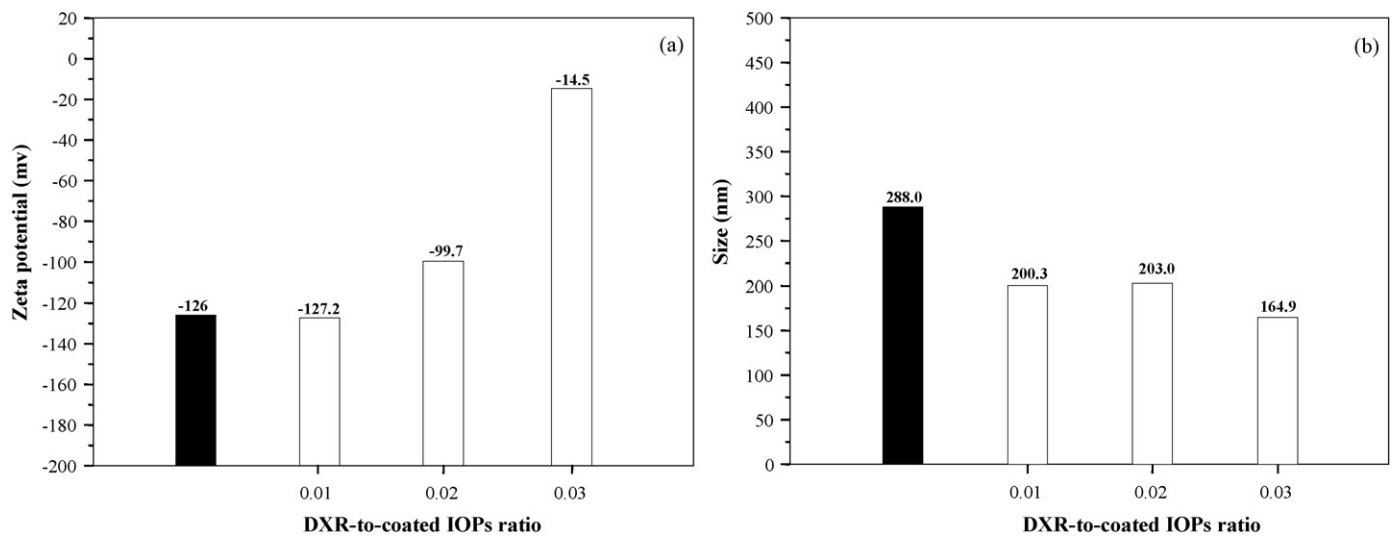


Fig. 6. Effects of DXR-to-coated IOPs ratio on zeta potential (a) and size (b) of gelatin-B coated IOPs before (■) and after (□) drug loading.

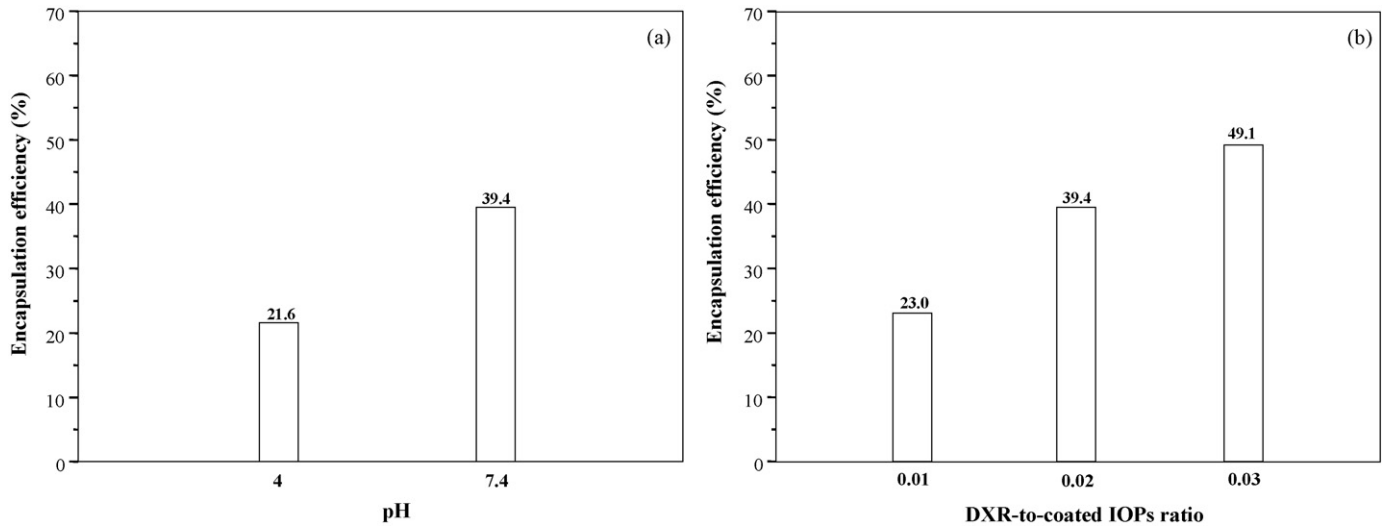


Fig. 7. Effects of pH (a) and DXR-to-coated IOPs (b) on encapsulation efficiency of gelatin B-coated IOPs.

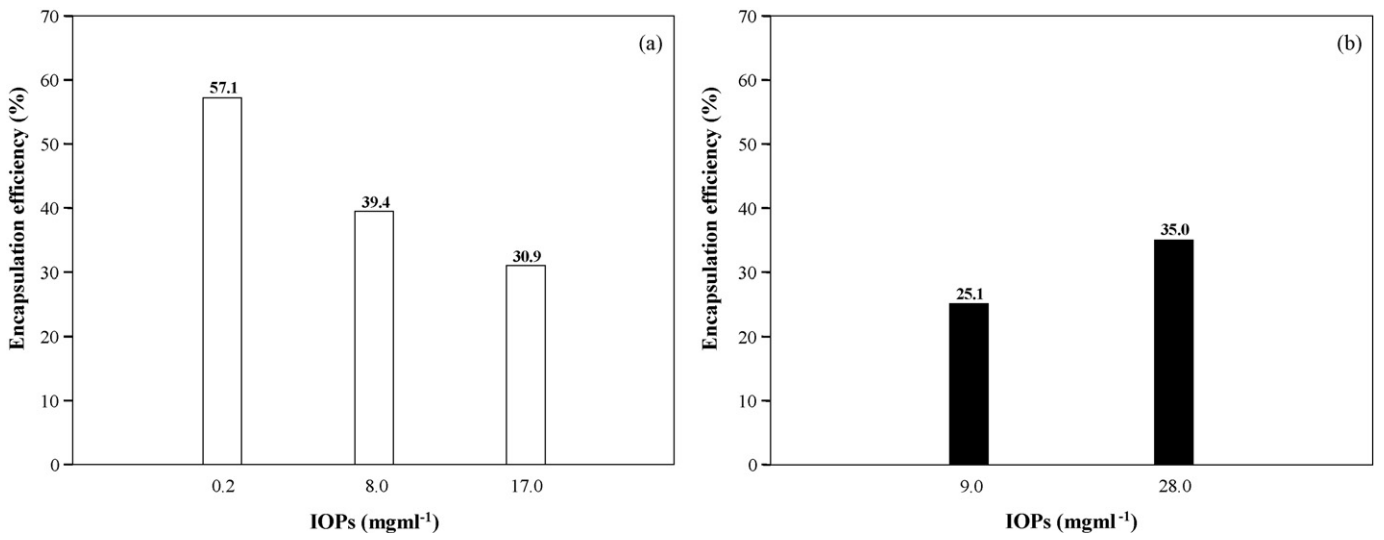


Fig. 8. Effects of IOPs concentration on encapsulation efficiency of gelatin B (a) and A (b) coated IOPs.

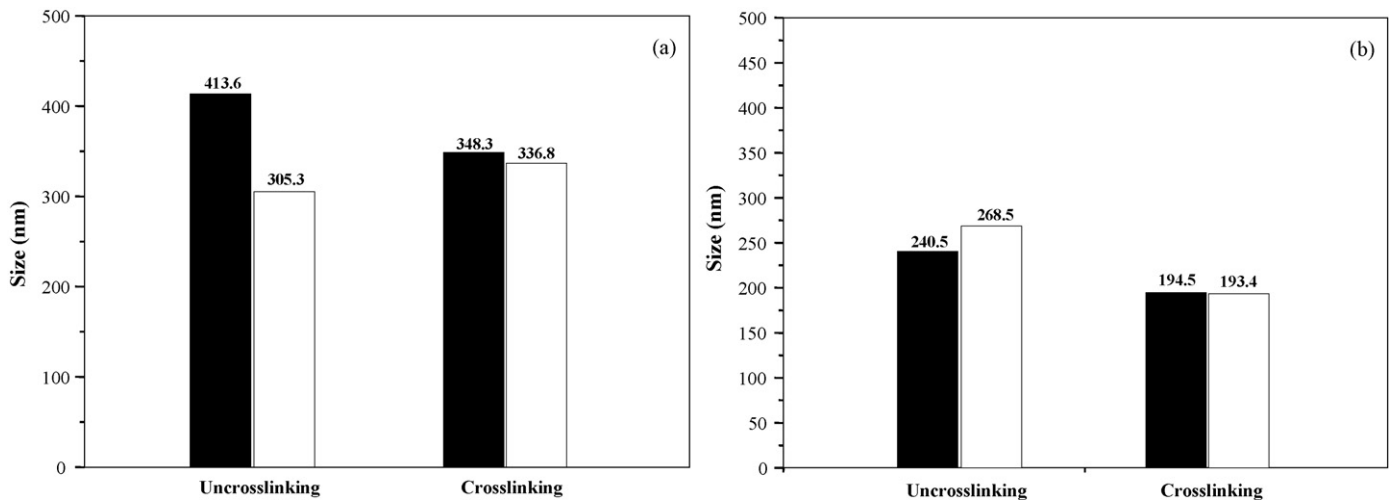


Fig. 9. Effects of desolvation and cross-linking on the size of gelatin B (a) and A (b) coated IOPs before (■) and after drug loading (□).

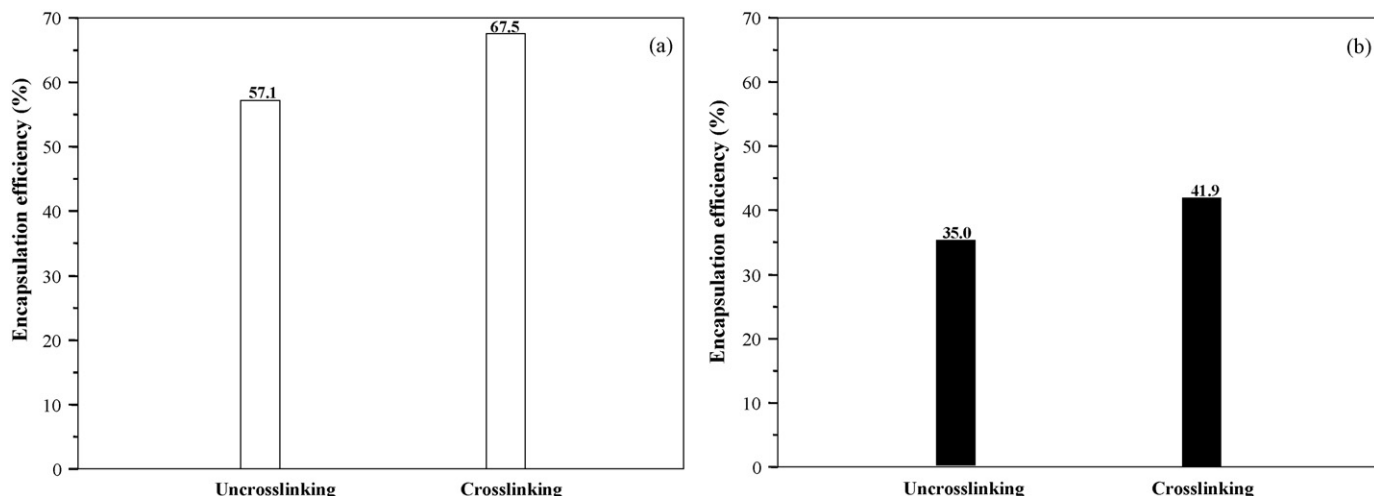


Fig. 10. Effects of drug loading technique on encapsulation efficiency of gelatin B (a) and A (b) coated IOPs.

However, the DXR release from gelatin B-coated IOPs was slow and controlled in basic as well as acidic release medium. In the early stage of 2 h, in the basic medium, release of only 11% of DXR occurred. The release continued for next 30 h leading to release of extra 21%, after which the release was very slow and insignificant. The release profile of DXR from the same carrier system, in acidic medium of pH 4, showed very fast release with almost 44% of burst release within 2 h of experiment. An extra 17% of drug released in eighth hour of experiment after which there was insignificant release. In conclusion, total 32% of drug released in 30 h of experiment from the coated IOPs in basic release medium while 61% of drug released in 8 h of experiment from the coated IOPs in acidic release medium.

The fast release profile at pH 4, can be justified because at this pH the carrier system (gelatin-coated IOPs) acquired positive charge, as shown by Fig. 4a, which resulted in weaker DXR to coated IOPs interaction, hence, very fast release upto 61% compared to basic medium (upto 32%) in 30 h (Fig. 11a). The burst release of the DXR, in the first 2 h, in both the acidic and basic release medium, corresponded to the weakly associated DXR in the carrier system, especially surface bound drug particles. A slow release observed after 2–30 h also cor-

responded the free DXR but those, which were trapped in coated IOPs, probably, by the gelatin layer. Rest of the unreleased DXR could be viewed as those strongly bound to the carrier system due to strong electrostatic bond.

3.3.2. In presence of enzyme

In order to evaluate the release of DXR fraction tightly linked to the carrier system (gelatin-coated IOPs), the donor solution was treated with proteolytic enzyme (trypsin) and release was continued as before. Fig. 11b suggested that there was a burst release of extra 23% of DXR in 5 h after enzyme addition, in basic medium. After that there was very slow release resulting in release of extra 20% in 127 h, after enzyme addition. The DXR release in acidic medium, however, did not show significant burst release (Fig. 11b). Since, large amount of DXR (upto 61%) was found to release before enzyme addition, it appeared that almost free DXR released before enzyme was added. However, there was slow release of DXR resulting in release of extra 34% in 127 h, after enzyme addition. In conclusion, there was extra 43 and 34% of drug release after enzyme addition in basic and acidic release medium, respectively. The release of DXR after enzyme addition shown in the medium of both

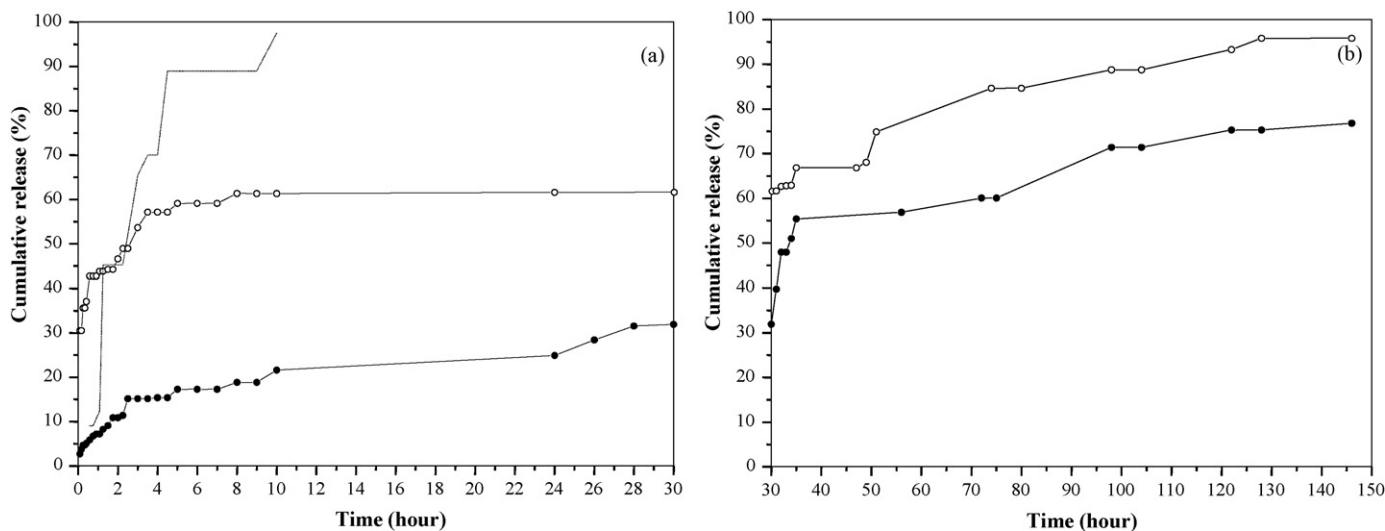


Fig. 11. Drug release profiles of gelatin B-coated IOPs in acidic (○), and basic (●) release medium of pH 4 and 7.4, respectively, in absence (a) and presence (b) of enzyme. Broken line represents the release profile of pure doxorubicin.

pH 4 and 7.4 corresponded to the DXR tightly bound to the coated IOPs. Upon enzymatic degradation, release of free or DXR-coupled coated particles with a molecular weight lower than 13,000 Da (cut-off value for the membrane) could take place from the dialysis bag.

Rapid drug release from the carrier in the vicinity of tumor vascular endothelial cells was considered effective in tumor regression (Needham et al., 2000). So, various triggering mechanisms had been described in the literature, including those that rely on changes in local microenvironment such as decreased pH (Drummond et al., 2000), presence of specific enzymes (Vermehren et al., 1998), and heat (Chiu et al., 2005). The pH responsive drug release profile shown by gelatin B-coated IOPs would make it an interesting candidate that would have potential application as a carrier system to attain pH-induced drug release of the loaded drug to the target site.

4. Conclusions

The ferrofluid of gelatin-coated IOPs showed physicochemical properties depending upon the IOPs, gelatin amount, and types of gelatin. The increase in surface charge of coated IOPs after drug loading indicated charge-induced adsorption of positive doxorubicin to negative coated IOPs. The increase or decrease in encapsulation efficiency of coated IOPs according to the surface charge of the coated IOPs also confirmed the involvement of drug-to-particle interaction in the drug-loading phenomenon. Furthermore, the carrier capacity of gelatin-coated IOPs were higher when loading process was done by desolvation/cross-linking technique compared to adsorption process only. The drug-loaded particles showed pH-triggered release of drug with higher release rate at lower pH of 4 compared to pH 7.4.

Acknowledgement

This research was supported by the Korean Research Foundation Grant Funded by the Korean Government (MOEHRD) (The Center for Healthcare Technology Development, Jeonju 561-756, Republic of Korea).

References

- Bajpai, A.K., Choubey, J., 2006. Design of gelatin nanoparticles as swelling controlled delivery system for chloroquine phosphate. *J. Mater. Sci.: Mater. Med.* 17, 345–358.
- Bele, M., Gaberscek, M., Dominko, R., Drogenik, J., Zupan, K., Komac, P., Kocovar, K., Musevic, I., Pejovnik, S., 2002. Gelatin-pretreated carbon particles for potential use in lithium ion batteries. *Carbon* 40, 1117–1122.
- Chang, M.C., Tanaka, J., 2002. FT-IR study for hydroxyapatite/collagen nanocomposite cross-linked by glutaraldehyde. *Biomaterials* 23, 4811–4818.
- Chiu, G.N.C., Abraham, S.A., Ickenstein, L.M., Ng, R., Karlsson, G., Edwards, K., Wasan, E.K., Bally, M.B., 2005. Encapsulation of doxorubicin into thermosensitive liposomes via complexation with the transition metal manganese. *J. Control. Rel.* 104, 271–288.
- Coester, C., Nayyar, P., Samuel, J., 2006. *In-vitro* uptake of gelatin nanoparticles by murine dendritic cells and their intracellular localization. *Eur. J. Pharm. Biopharm.* 62, 306–314.
- Cornell, R.M., Schwertmann, U., 2000. *The Iron Oxides: Structure, Properties, Reactions, Occurrence and Uses*, 2nd ed. Weinheim Wiley, p. 142.
- Drummond, D.C., Zignani, M., Leroux, J., 2000. Current status of pH-sensitive liposomes in drug delivery. *Prog. Lipid Res.* 39, 409–460.
- Engvall, E., Ruoslahti, E., 1977. Binding of soluble form of fibroblast surface protein, fibronectin, to collagen. *Int. J. Cancer* 20, 1–5.
- Gaihre, B., Aryal, S., Khil, M.S., Kim, H.Y., 2008. Encapsulation of Fe₃O₄ in gelatin nanoparticles: effect of different parameters on size and stability of the colloidal dispersion. *J. Microencapsul.* 25, 21–30.
- Gaihre, B., Aryal, S., Nasser, A.M.B., Kim, H.Y., 2008b. Gelatin stabilized iron oxide nanoparticles as a three dimensional template for the hydroxyapatite crystal nucleation and growth. *Mater. Sci. Eng. C* 28, 1297–1303.
- Gupta, A.K., Curtis, A.S.G., 2004. Lactoferrin and ceruloplasmin derivatized superparamagnetic iron oxide nanoparticles for targeting cell surface receptors. *Biomaterials* 25, 3029–3040.
- Gupta, A.K., Gupta, M., 2005. Synthesis and surface engineering of iron oxide nanoparticles for biomedical applications. *Biomaterials* 26, 3995–4021.
- Herman, T.S., 1983. Temperature dependence of adriamycin, cis-diamminedichloroplatinum, bleomycin, and 1,3-bis(2-chloroethyl)-1-nitrosourea cytotoxicity *in-vitro*. *Cancer Res.* 43, 517–520.
- Hone, J.H.E., Howe, A.M., Whitesides, T.H., 2000. Rheology of polystyrene latexes with adsorbed and free gelatin. *Colloids Surf. A: Physicochem. Eng. Aspects* 161, 283–306.
- Kamiyama, Y., Israelachvili, J., 1992. Effect of pH and salt on the adsorption and interactions of an amphoteric polyelectrolyte. *Macromolecules* 25, 5081–5088.
- Kamyshny, A., Toledano, O., Magdassi, S., 1999. Adsorption of hydrophobized IgG and gelatin onto phosphatidyl choline-coated silica. *Colloid Surf. B: Biointerf.* 13, 187–194.
- Kushibiki, T., Matsuoka, H., Tabata, Y., 2004. Synthesis and physical characterization of poly(ethylene glycol)-gelatin conjugates. *Biomacromolecules* 5, 202–208.
- Illes, E., Tombacz, E., 2006. The effect of humic acid adsorption on pH-dependent surface charging and aggregation of magnetite nanoparticles. *J. Colloid Interf. Sci.* 295, 115–123.
- Leo, E., Cameroni, R., Forni, F., 1999. Dynamic dialysis for the drug release evaluation from doxorubicin-gelatin nanoparticle conjugates. *Inter. J. Pharm.* 180, 23–30.
- Leo, E., Vandelli, M.A., Cameroni, R., Forni, F., 1997. Doxorubicin-loaded gelatin nanoparticles stabilized by glutaraldehyde: involvement of the drug in the cross-linking process. *Inter. J. Pharm.* 155, 75–82.
- Malmsten, M., 1998. Formation of adsorbed protein layers. *J. Colloid Interf. Sci.* 207, 186–199.
- Maria, G.C., Luigi, L., Claudia, C., Zhouhai, Z., 2002. Gelatin nanoparticles produced by a simple W/O emulsion as delivery system for methotrexate. *J. Mater. Sci.: Mater. Med.* 13, 523–526.
- Mironyuk, I.F., Gun'ko, V.M., Turov, V.V., Zarko, V.I., Leboda, R., Zieba, J.S., 2001. Characterization of fumed silicas and their interaction with water and dissolved proteins. *Colloids Surf. A: Physicochem. Eng. Aspects* 180, 87–101.
- Muniyandy, S., Kesavan, B., Gomathinayagam, M., Kalathil, S.P., 2004. Ultrasonically controlled release and targeted delivery of diclofenac sodium via gelatin magnetic microspheres. *Int. J. Pharm.* 283, 71–82.
- Needham, D., Anyarambhatla, G., Kong, G., Dewhirst, M.W., 2000. A new temperature-sensitive liposome for use with mild hyperthermia: characterization and testing in a human tumor xenograft model. *Cancer Res.* 60, 1197–1201.
- Petri, A.F., Chastellain, M., Jeanneret, L.J., Ferrari, A., Hofmann, H., 2005. Development of functionalized superparamagnetic iron oxide nanoparticles for interaction with human cancer cells. *Biomaterials* 26, 2685–2694.
- Roullin, V.G., Deverre, J.R., Lemaire, L., Hindre, F., Julienne, M.C.V., Vienet, R., Benoit, J.P., 2002. Anti-cancer drug diffusion within living rat brain tissue: an experimental study using [³H](6)-5-fluorouracil-loaded PLGA microspheres. *Eur. J. Pharm. Biopharm.* 53, 293–299.
- Shi, Y., Chow, G.M., 2004. Carboxyl group (–CO₂H) functionalized ferrimagnetic iron oxide nanoparticles for potential bio-applications. *J. Mater. Chem.* 14, 2781–2786.
- Tian, Y., Bromberg, L., Lin, S.N., Hatton, T.A., Tam, C.K., 2007. Complexation and release of doxorubicin from its complexes with pluronic P85-b-poly(acrylic acid) block copolymers. *J. Control. Rel.* 121, 137–145.
- Vermehren, C., Kiebler, T., Hylander, I., Callisen, T.H., Jorgensen, K., 1998. Increase in phospholipase A2 activity towards lipopolymer-containing liposomes. *Biochim. Biophys. Acta* 1373, 27–36.
- Weber, C., Coester, C., Kreuter, J., Langer, K., 2000. Desolvation process and surface characterisation of protein nanoparticles. *Int. J. Pharm.* 194, 91–102.
- Wiedemann, G.J., Robins, H.L., Katschinski, D.M., Mentzel, M., D'Oleire, F., Kutz, M., Wagner, T., 1997. Systemic hyperthermia and ICE chemotherapy for sarcoma patients: rationale and clinical status. *Anticancer Res.* 17, 2899–2902.
- Wilhelm, C., Billotey, C., Roger, J., Pons, J.N., Bacri, J.C., Gazeau, F., 2003. Intracellular uptake of anionic superparamagnetic nanoparticles as a function of their surface coating. *Biomaterials* 24, 1001–1011.
- Young, R., Ozols, F., Myers, C.E., 1981. The anthracycline antineoplastic drugs. *N. Engl. J. Med.* 305, 139–153.
- Young, S., Wong, M., Tabata, Y., Mikos, A.G., 2005. Gelatin as a delivery vehicle for the controlled release of bioactive molecules. *J. Control. Rel.* 109, 256–274.